

Binocular summation for reflexive eye movements

Christian Quaia

Laboratory of Sensorimotor Research,
National Eye Institute, National Institutes of Health,
Department of Health and Human Services,
Bethesda, MD, USA



Lance M. Optican

Laboratory of Sensorimotor Research,
National Eye Institute, National Institutes of Health,
Department of Health and Human Services,
Bethesda, MD, USA



Bruce G. Cumming

Laboratory of Sensorimotor Research,
National Eye Institute, National Institutes of Health,
Department of Health and Human Services,
Bethesda, MD, USA



Psychophysical studies and our own subjective experience suggest that, in natural viewing conditions (i.e., at medium to high contrasts), monocularly and binocularly viewed scenes appear very similar, with the exception of the improved depth perception provided by stereopsis. This phenomenon is usually described as a lack of binocular summation. We show here that there is an exception to this rule: Ocular following eye movements induced by the sudden motion of a large stimulus, which we recorded from three human subjects, are much larger when both eyes see the moving stimulus, than when only one eye does. We further discovered that this binocular advantage is a function of the interocular correlation between the two monocular images: It is maximal when they are identical, and reduced when the two eyes are presented with different images. This is possible only if the neurons that underlie ocular following are sensitive to binocular disparity.

threshold levels typical of our daily experience (Campbell & Green, 1965; Rose, 1980; Arditì, Anderson, & Movshon, 1981; Legge & Rubin, 1981; Legge, 1984a; Legge, 1984b; Anderson & Movshon, 1989; Cagenello, Arditì, & Halpern, 1993; Zlatkova, Anderson, & Ennis, 2001; Ding & Sperling, 2006; Meese, Georgeson, & Baker, 2006; Baker, Meese, & Georgeson, 2007; Hess, Hutchinson, Ledgeway, & Mansouri, 2007; Pineles, Velez, Yu, Demer, & Birch, 2014). Similarly, binocular vision improves neither smooth pursuit eye movements (González, Lillakas, Greenwald, Gallie, & Steinbach, 2014; Shanidze, Heinen, & Verghese, 2017) nor saccadic eye movements (Krauskopf, Cornsweet, & Riggs, 1960). In fact, thanks to our exquisite ability to exploit monocular depth clues, under monocular viewing we even maintain a vivid sensation of depth. Accordingly, most human activities, including operating a motor vehicle, can be carried out by monocularly blind subjects.

Introduction

The primary benefit of having two forward-facing eyes is enhanced depth perception. In principle, combining signals from both eyes could improve other functions, such as form detection. However, a large body of psychophysical research has revealed that, whereas at very low contrasts (around perception threshold) binocular vision confers a significant advantage in contrast sensitivity and visual acuity, this vanishes quickly as contrast is increased to the supra-

Neural processing of binocular stimuli starts in primary visual cortex (area V1 in primates), where most neurons receive inputs from both eyes, and are more strongly activated by their preferred binocular stimulus than by their preferred monocular stimulus (Barlow, Blakemore, & Pettigrew, 1967; Pettigrew, Nikara, & Bishop, 1968; Poggio & Fischer, 1977; Prince, Pointon, Cumming, & Parker, 2002), at all contrast levels. Accordingly, perceptual invariance between monocular and binocular presentations requires either selective pooling of V1 responses, or additional processing beyond V1. Other behavioral responses might not share

Citation: Quaia, C., Optican, L. M., & Cumming, B. G. (2018). Binocular summation for reflexive eye movements. *Journal of Vision*, 18(4):7, 1–17, <https://doi.org/10.1167/18.4.7>.



such pooling/processing, and thus might reveal a clear binocular advantage. Anecdotal reports (Miles, Kawano, & Optican, 1986; Inoue, Takemura, Kawano, & Mustari, 2000) indicate that in monkeys reflexive eye movements known as ocular following responses (OFRs), supported primarily by the dorsal visual pathway (Miles, 1997; Miles, 1998; Kawano, 1999; Masson, 2004; Miles, Busetini, Masson, & Yang, 2004; Takemura, Murata, Kawano, & Miles, 2007), are stronger for binocular than monocular high contrast stimuli, suggesting that OFRs might exhibit binocular summation.

To test this hypothesis, we recorded OFRs induced by brief presentations of drifting sinusoidal gratings, shown monocularly or binocularly, in three human subjects. We found that responses to binocular stimuli are always significantly larger, with a binocular gain that can be as high as 10, and never lower than 2 (corresponding to linear summation), even at high contrast. This is the first demonstration of strong binocular summation at all contrasts. Using one-dimensional noise patterns we further demonstrated that binocular summation is sensitive to the interocular correlation between the patterns seen by the two eyes, indicating that the OFR is mediated by disparity-selective neurons.

Materials and methods

Subjects

Three human subjects (all male, two naive; ages 22–55) participated in the study. All subjects had normal or corrected-to-normal visual acuity and normal stereoacuity (evaluated using the Titmus, Randot, and Worth tests). Experimental protocols were approved by the Institutional Review Board concerned with the use of human subjects, and informed consent was obtained from all subjects. The study was carried out in accordance with the Code of Ethics of the World Medical Association (Declaration of Helsinki); all personal identifiable information was handled in accordance with NIH privacy directives.

Apparatus

Subjects sat in a dark room, with their head stabilized using chin and forehead padded supports and a headband. Binocular stimulation was delivered using a custom built Wheatstone mirror stereoscope. The two CRT monitors (GDM-FW900; Sony, Tokyo, Japan) composing the stereoscope were viewed through 45° mirrors, arranged so that the optical distance of the

monitors and the apparent distance of the binocular image seen through the mirrors were identical (521 mm). Each monitor screen covered 50° (H) by 32° (V) of visual angle, was set at a resolution of 1,280 columns by 800 rows, and a refresh rate of 140 Hz. Only the red channel was used, to minimize persistence (1 ms rise time, 4 ms fall time) and guarantee the absence of motion streaks (DeAngelis & Newsome, 2004). A single video card (Geforce GTX 580 Classified; EVGA, Brea, CA) was used to drive both monitors. The refresh timing of the two monitors was tightly synchronized, with the left eye image consistently preceding the right eye image by less than 50 μ s. Luminance linearization was performed by interpolation following dense luminance sampling (using an LS100 luminance meter; Konica Minolta, Tokyo, Japan), independently for each monitor.

Horizontal and vertical positions of both eyes were recorded using an electromagnetic induction technique (Robinson, 1963). A scleral search coil embedded in a silastin ring (Skalar, the Netherlands; Collewijn, van der Mark, & Jansen, 1975) was placed in each eye following application of topical anesthetic (proparacaine HCl). Each coil output (sampled at 1,000 Hz) was calibrated at the beginning of each recording session by having the subject look at targets of known eccentricity. Peak-to-peak noise levels resulted in an uncertainty in eye position recording of less than 0.03°.

The experiment was controlled by two computers, one, running the Real-time EXperimentation software package (Hays, Richmond, & Optican, 1982), to manage the workflow and acquire and store the data, and the other, directly connected to the monitors, to generate the required visual stimuli in response to REX commands. This was accomplished using the Psychophysics Toolbox 3.0.8, a set of MATLAB (MathWorks, Natick, MA) scripts and functions (Brainard, 1997).

Behavioral paradigm: Ocular following

Trials were presented in blocks; each block contained one trial for each stimulus condition. All conditions within a block were randomly interleaved. Each trial began with the appearance of a binocular central fixation cross on a blank, mid-luminance (6.0 cd/m²), background. The subject was instructed to look at the center of the cross, and avoid making saccadic eye movements. After the subject maintained fixation within a small (1° on the side) invisible window around the fixation point for 800–1,100 ms, the fixation cross disappeared, and the visual stimulus sequence was presented for 170 ms. Subsequently the screen was blanked (again at mid-luminance), signaling the end of the trial. After a short intertrial interval, a new trial was started. If the subject blinked, or if saccades were

detected during the stimulus presentation epoch, the trial was discarded and repeated within the block.

Behavioral paradigm: Perception

Trials were presented in blocks; each block contained one trial for each stimulus condition. All conditions within a block were randomly interleaved. A two-interval forced choice (2IFC) paradigm with constant stimuli was employed. Each trial began with the appearance of a central fixation cross on a blank, mid-luminance (6.0 cd/m^2), background. The subject was instructed to fixate the cross. After 800–1,100 ms, the fixation cross disappeared, and a first stimulus sequence (170 ms) was presented. At the end of presentation, a tone was emitted by a speaker and the screen was blanked (again at 6.0 cd/m^2) for 500 ms. A second stimulus sequence (170 ms) was then presented. Finally, the screen was blanked (again at 6.0 cd/m^2), and the subject had unlimited time to report, by pressing one of two buttons, whether the stimulus with higher apparent contrast was presented in the first or second interval. Once a response was recorded, a new trial was initiated.

Visual stimuli

All the stimuli had a mean luminance of 6.0 cd/m^2 , and they were presented within a large aperture, centered on the screen. Outside the aperture the screen was blank, at mid-luminance. Two main classes of visual stimuli were used.

The first class of stimuli consisted of horizontal sinusoidal gratings, presented within a circular aperture (28° diameter). All gratings had a spatial frequency (SF) of 0.25 cpd, appeared suddenly and drifted upward or downward for 170 ms within the aperture, with a temporal frequency (TF) of 17.5 Hz. SF and TF were chosen, based on previous studies, to maximize the magnitude of the OFRs. The Michelson contrast of the grating was varied between 2.5% and 80% in one-octave increments. The stimulus was seen by either one eye only (“monocular” condition), while the other saw a mid-luminance blank screen, or by both eyes (“binocular” condition). In one subject (indicated as N3a), vertical stimuli drifting horizontally were also used. In that experiment, luminance was also higher (20.8 cd/m^2) and all three guns of the CRT monitors were used.

The second class of patterns consisted of horizontal 1D random line stimuli (RLS), presented within a 28° diameter circular aperture. Each RLS was obtained by randomly assigning either a high or a low luminance value (symmetric around mean luminance) to each

consecutive pair of rows of pixels (0.08°); it was moved at a speed of approximately $40^\circ/\text{s}$. Motion of the RLS was simulated by shifting either up or down (by an integer number of rows at each frame) a pattern larger than the screen behind the fixed aperture (i.e., the stimulus did not “wrap around”). The Michelson contrast, which is also equal to the root mean square (RMS) contrast for binary RLS, was varied between 2.5% and 80% in one octave increments. The two eyes could either see the same RLS (“binocular-same” condition), two different (uncorrelated) RLS (“binocular-different” condition), or the RLS could be presented to one eye while the other saw a mid-luminance blank screen (“monocular” condition).

In one subject we also ran an additional experiment in which drifting low-pass filtered horizontal RLS were presented. The gain of the filter was one below 0.375 cpd and zero above 0.75 cpd; the transition followed a raised-cosine function. The RMS contrast of the stimuli was varied between 1.5% and 24%. With non-binary RLS, RMS contrast is lower than, and limited by, Michelson contrast, but there is no fixed relationship between the two. We imposed a fixed value of RMS contrast (as opposed to Michelson contrast) because with noise stimuli RMS contrast has been shown to be a better indicator of stimulus strength (Moulden, Kingdom, & Gatley, 1990; Kukkonen, Rovamo, Tiippana, & Näsänen, 1993). The two eyes either saw the same RLS (“binocular-same” condition), two different (uncorrelated) RLS (“binocular-different” condition), or contrast-reversed (anti-correlated) versions of the same RLS (“binocular-opposite” condition).

Statistical analysis

All the measures reported here are based on eye velocity. The calibrated eye position traces (see Apparatus) were differentiated using a 21-point finite impulse response (FIR) acausal filter (47 Hz cutoff frequency). Trials with saccadic intrusions and unstable fixation that went undetected at run time were removed using an automatic procedure aimed at detecting outliers (Quaia, Optican, & Cumming, 2013). Average temporal profiles, time-locked to stimulus onset, were then computed over the remaining trials, separately for each stimulus condition. To remove the effect of components of the eye response related to the disengagement of fixation (Bostrom & Warzecha, 2010; Quaia, Sheliga, Fitzgibbon, & Optican, 2012), we report not the raw OFR, but rather the difference between the OFRs to upward and downward motion directions (rightward and leftward for N3a). The traces and measurements reported here are thus based on the difference between the average responses to stimuli

containing motion energy in opposite directions. The strength of the OFR was quantified by computing, for each condition, the average difference eye speed in a time window that started at the latency of the response. The latency, which is a function of contrast, was defined as the time at which the difference eye speed became significantly ($p < 0.05$) different from zero, and was determined using a non-parametric bootstrap-based technique (Quaia, Sheliga, Optican, & Cumming, 2013). Latencies were initially computed separately for each stimulus condition. Inspection of the results revealed that monocular contrast is the prime determinant of latency. A lack of significant difference between the latency of OFRs to high contrast random dot stimuli presented monocularly or binocularly had also been previously reported in monkeys by others (Miles et al., 1986; Inoue et al., 2000). Because binocular responses are considerably larger, and thus provide a more reliable estimate of latency, we then used the latencies extracted from the binocular conditions (or “binocular-same” conditions for RLS stimuli) for the monocular responses as well (Figure 1). This has the added benefit of comparing monocular and binocular responses in identical time windows. The duration of the time window over which speed was averaged was equal to the latency of the response to the highest contrast stimulus (which varied between 67 and 75 ms across subjects). This ensured that the time window over which we measured the OFR was always restricted to the open-loop period (the period before motion of the eyes introduces a difference between motion on the display and motion on the retina that can affect the OFRs), and that measures from different contrast levels were computed over windows of the same duration.

All statistical analyses, including computations of standard errors and significance values, were carried out using non parametric, bootstrap-based methods (Efron, 1982). A detailed description of the bootstrap procedures used can be found elsewhere (Quaia et al., 2012).

Model fitting

To quantify the relationship between the contrast of the stimulus and the strength of the OFR (the contrast response function, CRF), we measured the average eye speed in a time window, and used a Naka–Rushton function (also known as the Michaelis–Menten equation) to fit the CRF:

$$\mathcal{R}(c_s) = A \frac{c_s^n}{c_s^n + c_{50}^n} \quad (1)$$

where c_s is the contrast of the stimulus, A is a gain factor (which for the OFRs takes into account also the

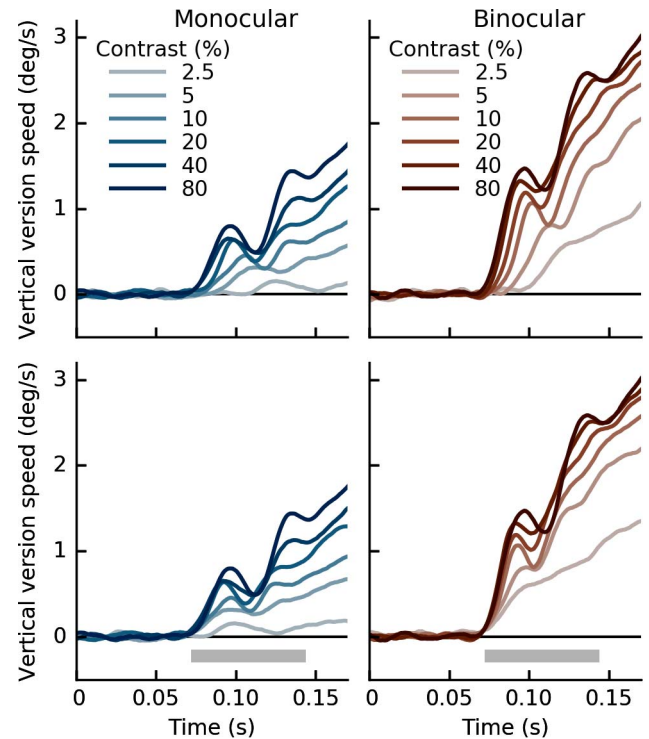


Figure 1. Monocular and binocular OFRs. The sudden onset of a drifting horizontal sinusoidal grating (0.25 cpd SF, 17.5 Hz TF) induces a short-latency (approximately 70 ms in humans) vertical OFR. Both the magnitude and the latency of the responses vary with the contrast of the stimulus (top row). For any given contrast, binocular stimuli induce much stronger responses. To estimate response strength as a function of contrast without the additional confound of latency changes, the responses can be aligned in time with the response to the highest contrast stimulus, based on the latency of binocular responses (bottom row). The strength of the response is then quantified by computing the average eye speed in a time window that goes from the onset of the response to twice the latency (open-loop period), indicated here with a gray bar above the abscissa. Data from subject N1.

sensorimotor gain, and thus varies widely across subjects), n determines the slope of the curve, and c_{50} is the semi-saturation contrast (i.e., the contrast at which the response drops to $A/2$) and places the curve along the c_s axis. Monocular and binocular conditions were fitted separately, with c_s indicating monocular and binocular contrast, respectively.

Function fitting was performed using a simplex optimization algorithm in Python (using the numpy library). We did not minimize the summed squared error, but rather the χ^2 measure:

$$\chi^2 = \sum_i \left(\frac{y_i - \hat{y}_i}{s_i} \right)^2$$

where, for each experimental condition i , we indicate

with y_i the mean OFR across trials, s_i the standard error of y_i , and \hat{y}_i the value of the fitted function for that condition. More consistent responses are thus weighted more heavily in determining the quality of a given fit, maximizing the likelihood of the model given the data.

The Naka–Rushton function provides descriptive fits, but offers no insights into how the differences between monocular and binocular OFRs might arise. We thus developed a simple cascade model, in which at the first stage each monocular input is passed through identical Naka–Rushton functions (representing monocular gain control mechanisms), whose outputs converge on a binocular stage, which is also modeled using a Naka–Rushton function (representing a binocular gain control mechanism). Because the gain parameters in the two stages are redundant, in the first stage we simply imposed a unitary gain. The basic model (illustrated in Figure 4A) has thus five parameters, and is described by the following equations:

$$\begin{aligned} y_{RE} &= \frac{c_{RE}^n}{c_{RE}^n + c_{50}^n} \\ y_{LE} &= \frac{c_{LE}^n}{c_{LE}^n + c_{50}^n} \\ y &= y_{RE} + y_{LE} \\ z &= G \frac{y^m}{y^m + y_{50}^m} \quad (2) \end{aligned}$$

where c_{RE} (c_{LE}) is the contrast of the stimulus presented to the right (left) eye. Model fitting was again carried out by minimizing χ^2 . The model was used only to fit the OFRs induced by sinusoidal drifting gratings. It was fitted separately to each subject's data by using a simplex optimization algorithm in Python to find the set of five model parameters that resulted in the best match (i.e., minimal χ^2) between the subject's OFR and the model output z , across all monocular and binocular conditions at once. To compare the model performance to that of the Naka–Rushton fits one then needs to compare the χ^2 for the model to the sum of the χ^2 values for the Naka–Rushton fits to the monocular and binocular data.

Results

Binocular summation with sinusoidal gratings: OFRs

We recorded the vertical eye movements induced by a drifting horizontal sinusoidal grating (SF = 0.25 cpd, TF = 17.5 Hz), which appeared suddenly on a mid-luminance background, and started drifting immedi-

ately (upward or downward, for 170 ms). The stimulus was presented either to only one eye (while the other eye saw a mid-luminance blank screen) or to both eyes, and its Michelson contrast was varied between 2.5% and 80%.

In Figure 1 we show the time course of the vertical version velocity (i.e., the mean vertical velocity of left and right eye) in response to monocular and binocular stimuli, in one subject. For monocular stimuli, the responses to the left-eye-only and right-eye-only stimuli were averaged. In the top row, responses are shown time-locked to the onset of the stimulus. In the bottom row the responses to 2.5%–40% contrast have been shifted back in time to bring them in alignment with the 80% contrast response. The time shifts were computed based on the latency of the binocular responses (first time when each response becomes significantly larger than zero), and then applied to both binocular and monocular responses. We chose to base our alignment on binocular responses because monocular responses were much smaller, making it difficult to reliably estimate their latency, especially at low contrasts. Note that the monocular responses are very well aligned (with the exception of the response to the 2.5% stimulus in this case). This held true for all subjects and in all experiments.

Four aspects of the data stand out: (1) The magnitude of responses increases with increasing contrast; (2) The latency of responses decreases with increasing contrast; (3) At each contrast level, binocular responses are larger than monocular responses; and (4) The binocular advantage is dramatic, e.g., a 5% binocular stimulus induces a stronger, albeit much delayed, OFR than an 80% monocular stimulus. The first two results were expected, and replicate previous observations (Miles et al., 1986; Gellman, Carl, & Miles, 1990; Sheliga, Chen, Fitzgibbon, & Miles, 2005; Miura et al., 2006; Barthelemy, Perrinet, Castet, & Masson, 2008). The relationship between monocular and binocular responses across contrast levels is the focus, and the novel contribution, of our study.

To quantify the strength of the response we computed the average eye speed of these time-shifted responses in a fixed time window (duration between 67 ms and 75 ms across subjects), indicated with a horizontal bar above the time axis in Figure 1. From here on we focus on this measure, which we simply call the OFR. The relationship between contrast and the OFR in our three subjects is shown in Figure 2, separately for monocular (blue) and binocular (orange) stimuli. In all subjects, responses to binocular stimuli were not only much larger than those to monocular stimuli of the same contrast, but also larger than what would be expected under linear summation (twice the monocular response, dashed blue line). Naka–Rushton functions (Equation 1) fitted to the data are also shown

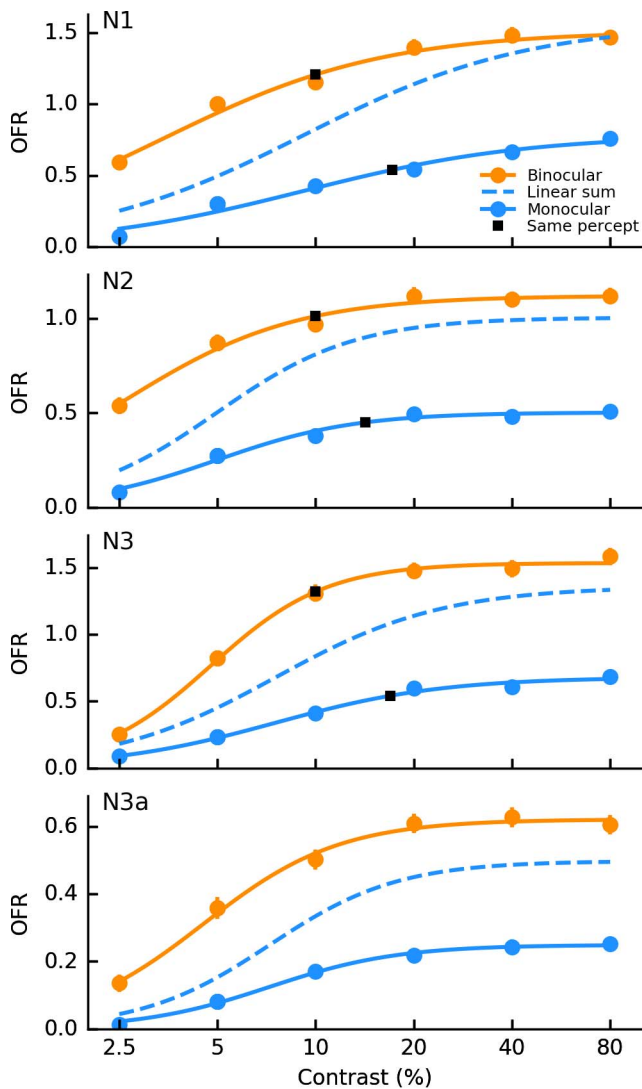


Figure 2. Contrast tuning of OFRs to monocular and binocular drifting sinusoidal gratings. OFRs increased monotonically with the contrast of the stimulus, but saturated at intermediate and high contrasts. At all contrasts the responses to binocular stimuli (orange) were at least twice as large (dashed blue) as the responses to monocular stimuli (solid blue). For subject N3, responses to stimuli that differed in orientation of the gratings, mean luminance, and color of the illumination, are also reported for comparison (N3a). Both mean and *SEM* bars are shown, but the *SEM* bar is often smaller than the marker used for the mean. Naka–Rushton fits to the data are shown; values for the parameters and goodness-of-fit measures are listed in Table 1. Black squares indicate binocular and monocular stimuli that subjects perceived as having the same contrast (Figure 5B).

(solid lines), with parameter values and goodness-of-fit measures for the fits listed in Table 1. Black squares indicate monocular and binocular stimuli that were perceived by our subjects as having the same contrast, based on experiments described later on. With subject N3 we also replicated the experiment using vertically (instead of horizontally) oriented stimuli, higher mean

luminance (20.8 cd/m^2 instead of 6 cd/m^2), and grayscale instead of red-scale illumination. The results (indicated as N3a in Figure 2) are remarkably similar, ruling out these factors as contributing to the phenomena reported here.

Because we reported the average speed of the two eyes, these results are also compatible with the hypothesis that each eye simply tracked the stimulus it saw (i.e., that under monocular conditions only one eye moved). We ruled this out by comparing the speed of the right and left eyes under monocular and binocular conditions (Figure 3). When the stimulus was presented only to the right eye (Figure 3A), the mean vertical (horizontal for N3a) speed (computed over the same time windows used for Figure 2) of the right (abscissa) and left (ordinate) eyes were very similar, for all subjects and across all contrasts tested. The same held true when stimuli were shown to the left eye only (Figure 3B). In both cases both eyes moved when only one eye saw the stimulus, and their mean speed was highly correlated (Pearson's $r > 0.996$); there was a modest tendency for the eye seeing the stimulus to move slightly faster than the other eye, especially in subject N1. Under binocular stimulation (Figure 3C), there was again a very strong correlation between the speed of the two eyes (Pearson's $r > 0.997$); in subjects N1 and N3 the right eye moved consistently faster, in N2 and N3a the left eye did, but again the differences were very small. Since the three panels share the same scale, it is also immediately apparent that each eye moved much faster under binocular than monocular conditions. The results cannot thus be explained by a disconjugate drive: Even under monocular stimulation, the OFRs were largely conjugate, with only a small vergence component, just like saccadic and smooth pursuit eye movements. This holds for both vertically and horizontally drifting stimuli (i.e., horizontal and vertical vergence appears to be equally stable during OFRs). This also indicates that recording the position of both eyes is not necessary to estimate the ratio between responses to monocular (averaging the movements induced by left eye only and right eye only presentations) and binocular stimuli of the same contrast. In Figure 3D we demonstrate this by computing this ratio based on the right eye speed only (abscissa) and on the version speed (ordinate). The two measures are highly correlated (Pearson's $r > 0.99$), and never significantly different.

We just showed that the mean eye speed induced in the two eyes was highly correlated across stimuli, regardless of whether one or both eyes saw the target. As an aside, we wondered whether this tight correlation also held at the trial-by-trial level. We thus computed Pearson's correlation between the mean speed in each eye in individual trials, over multiple presentations of the same stimulus. We found that it was always very

Figure	Subject	Stimulus	A	n	c_{50}	χ^2	r^2
2	N1	Monocular	0.78	1.27	9.19	19.11	0.977
		Binocular	1.51	1.27	3.39	6.40	0.984
	N2	Monocular	0.50	2.05	4.99	6.18	0.985
		Binocular	1.12	1.64	2.56	3.76	0.984
	N3	Monocular	0.68	1.69	7.55	3.40	0.992
		Binocular	1.54	2.46	4.78	1.64	0.997
N3a	Monocular	0.25	2.21	7.23	0.85	0.996	
	Binocular	0.62	2.08	4.52	2.17	0.994	
6	N1	Monocular	0.78	1.06	20.44	12.60	0.980
		Bin-Same	1.10	1.56	3.61	10.60	0.922
		Bin-Diff	1.01	0.92	12.20	9.18	0.969
	N2	Monocular	0.44	2.36	12.87	1.41	0.997
		Bin-Same	0.75	3.27	4.54	9.04	0.911
		Bin-Diff	0.60	2.10	7.50	0.21	0.999
	N3	Monocular	0.68	1.78	16.47	24.92	0.973
		Bin-Same	1.46	1.80	9.21	2.47	0.997
		Bin-Diff	1.20	1.38	20.31	2.71	0.997
7	N3	Bin-Same	1.82	1.92	2.50	5.72	0.983
		Bin-Diff	1.30	2.17	3.42	4.29	0.987
		Bin-Opp	1.02	1.57	6.67	2.69	0.987

Table 1. Contrast tuning curves: Naka–Rushton fits.

high, ranging (across subjects) between 0.84 and 0.89 when an 80% contrast binocular stimulus (i.e., the stimulus inducing the largest responses) was presented, and between 0.81 and 0.88 when a 2.5% monocular stimulus (i.e., the stimulus inducing the weakest responses) was presented. When all the trials collected, regardless of stimulus, were pooled together, the correlation varied between 0.80 and 0.84. Thus, even the trial-by-trial noise is highly correlated (i.e., conjugate) between the two eyes in OFRs. This implies that

most of the trial-by-trial variability is a real property of the eye movements, not merely instrumental noise.

Since OFRs can be affected by the history of visual stimulation (Taki, Miura, Tabata, Hisa, & Kawano, 2009), we compared monocular and binocular responses separately on the subsets of trials that were preceded by higher and lower stimulus contrast. We found no significant differences in binocular gain (not shown), ruling out any effect of short-term adaptation on our results.

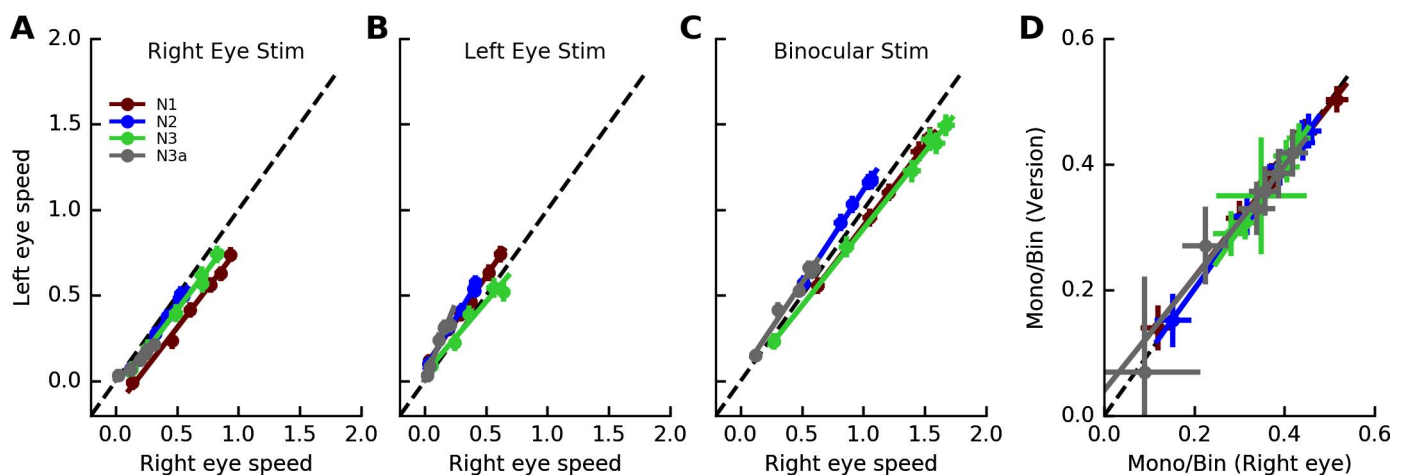


Figure 3. Monocular and binocular OFRs are conjugate. Whether the drifting grating was seen only by the right eye (A), only by the left eye (B), or by both eyes (C), the right (abscissa) and left (ordinate) eyes moved at very similar speeds, with binocular stimuli inducing stronger OFRs. The ratio between monocular and binocular responses (D) was the same whether it was computed based on the speed measured in one eye or the average speed of the two eyes. Both mean and SEM bars are shown. Type II regression lines are also shown.

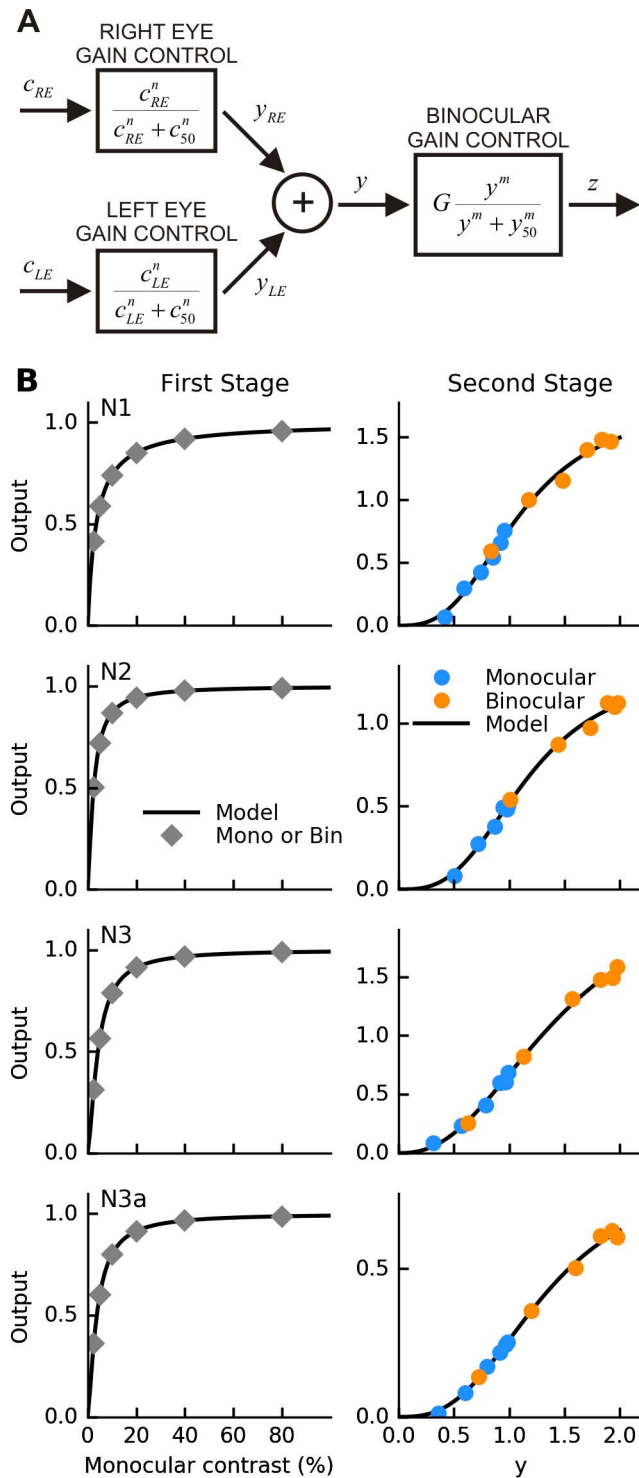


Figure 4. Modeling monocular and binocular OFRs. (A) The data was fitted using a two-stage cascade model, in which contrast gain control is exerted at both monocular and binocular levels. The model has five parameters, two in the first stage, and three in the second. (B) Fits to the data shown in Figure 2. In the left column, the predicted output of the first (monocular) stage as a function of the contrast of the stimulus is shown. Note that, unlike in Figure 2, a linear scale is used for the abscissa. In the right column, the output of the second stage as a function of its

Binocular summation with sinusoidal gratings: A simple model

To gain some insights into how such a strong enhancement for binocular stimuli might emerge, we fitted a simple two-stage model (Figure 4A) to the data. The contrast of the stimulus shown to each eye was fed to a first stage having a nonlinear input-output relationship described by a Naka–Rushton function. The outputs of the first stage for the left and right eyes were then summed. Finally, the resulting signal was fed to a second stage, also characterized by a Naka–Rushton input-output relationship (Equation 2). Model parameters were selected to best match the output of the second stage to the OFRs, across all monocular and binocular conditions at once.

The model fitted the data from each subject remarkably well (Figure 4B, one row per subject; parameter values and goodness-of-fit measures are listed in Table 2). The input to the first stage is monocular stimulus contrast. In the left column, we show the input–output relationship of the first stage (black); gray diamond symbols highlight the output of the first stage for the contrast levels that were tested in our experiment. Note that because a linear scale is used, the Naka–Rushton functions shown here appear more compressive than those in Figure 2, where a logarithmic scale was used for the abscissa, but this is deceiving (as can be inferred by comparing values for n and c_{50} in Tables 1 and 2). In the right column we show the input–output relationship of the second stage (black). The input to the second stage (y) is the sum of the outputs of the two first (monocular) stages (Equation 2), and it thus equals the location along the ordinate of the diamonds in the left column for monocular stimuli (blue), and twice that value for binocular stimuli (orange). The position along the ordinate of the symbols is equal to the OFRs shown in Figure 2.

The input–output relationships of the first and second stage are consistent across subjects. The first stage is compressive, with the output saturating for contrasts above 20%; the second stage is instead expansive at low and intermediate inputs, and only slightly compressive at large inputs. These properties are compatible with the strong contrast normalization observed in magnocellular neurons in the retina and LGN (Derrington & Lennie, 1984; Kaplan & Shapley, 1986; Sclar, Maunsell, & Lennie, 1990; Benardete,

input (sum of the outputs of the two monocular stages) is shown, together with OFRs for monocular (blue) and binocular (orange) stimuli (both mean and SEM bars are shown). Black lines show the input-output Naka-Rushton relationship of the two stages. Parameter values and goodness-of-fit measures are listed in Table 2.

Subject	n	c_{50}	G	m	y_{50}	χ^2	r^2
N1	1.00	3.51	1.77	2.82	1.10	25.14	0.993
N2	1.35	2.48	1.33	2.97	1.16	10.08	0.995
N3	1.51	4.21	2.34	2.37	1.46	8.34	0.997
N3a	1.41	3.75	0.83	2.76	1.33	2.98	0.997

Table 2. Contrast tuning curves: Two-stage model fits.

Kaplan, & Knight, 1992; Kremers, Silveira, & Kilavik, 2001; Solomon, White, & Martin, 2002; Webb et al., 2002; Priebe & Ferster, 2006; Solomon, Lee, & Sun, 2006; Alitto & Usrey, 2008; Camp, Tailby, & Solomon, 2009; Alitto, Moore, Rathbun, & Usrey, 2011), where neurons are monocular, and with the proposal that cortical areas, where most neurons receive inputs from both eyes, contribute to contrast normalization mostly by virtue of their (typically expansive) output nonlinearities (Albrecht & Geisler, 1991).

If we were to identify the first stage of our model with the LGN, and the second stage with cortex, the model could then be used to predict values of c_{50} measured experimentally in the LGN (c_{50} in Table 2), and in cortex (given the high similarity of the model and Naka–Rushton fits to the data, approximately equal to c_{50} in Table 1). Notably, our model would then predict that c_{50} in visual cortex is different for monocular and binocular stimuli. For binocular stimuli, our model predicts that c_{50} should be very similar when measured at the output of the LGN and cortex; with monocular stimuli it is instead predicted to be higher in cortex. However, magnocellular neurons in cortex are reported to have a lower c_{50} than magnocellular neurons in the LGN (Sclar et al., 1990), indicating that caution must be taken in making parallels between the model stages and neural structures. Nonetheless, we will later show that OFRs might be mediated by a small subset of cortical neurons, and thus direct comparisons with population averages might not be appropriate (see Discussion).

Modeling of perceptual binocular summation has a long history, and it might then be asked why we did not simply use one of the models developed in that context. In fact, our model is a slimmed down version of the two-stage gain control model used for perceptual summation (Meese et al., 2006). Compared to that model, we used a single exponent for the numerator and denominator at both the first and second stages (reducing the number of parameters), and omitted the interocular suppression term at the first stage. The latter accounts for the lack of binocular summation observed with perception, but, because of their strong binocular summation, it is not necessary for the OFRs. It must be stressed that our results do not exclude the presence of weak interocular suppression even for OFRs, since a more expansive nonlinearity at the second stage could overcome it. Models with attenu-

ated suppression from the other eye (Kingdom & Libenson, 2015) are thus not incompatible with OFRs. To test for the presence of interocular suppression, stimuli with unequal contrast in the two eyes need to be used. Because contrast affects not only the magnitude but also the latency of the response (see Figure 1), such data must be fitted with a dynamic model.

Binocular summation with sinusoidal gratings: Perception

The results that we have outlined so far are at odds with what has been reported about contrast perception of monocular and binocular stimuli: To normal subjects, high-contrast stimuli viewed through one or two eyes do not appear very different, in term of either luminance, contrast, or sharpness (Campbell & Green, 1965; Rose, 1980; Arditi et al., 1981; Legge & Rubin, 1981; Legge, 1984a; Legge, 1984b; Anderson & Movshon, 1989; Cagenello et al., 1993; Zlatkova et al., 2001; Ding & Sperling, 2006; Meese et al., 2006; Baker et al., 2007; Hess et al., 2007; Pineles et al., 2014). In stark contrast, in our subjects binocular stimuli induced OFRs that were at least twice as large as those induced by monocular stimuli, regardless of contrast. Inspection of Figure 2 reveals that a 80% contrast monocular stimulus induced a weaker OFR than a 10% binocular stimulus (which is quite dim). It would thus seem that perception and ocular following obey completely different rules in terms of binocular summation. There is however a potential flaw in this line of reasoning: The stimuli used for perceptual experiments are very different from the ones we used to record OFRs. In typical psychophysical experiments, the stimuli are much smaller, of much higher SF, static, and are usually present on the screen for longer times. Any of these differences might in principle explain the discrepancy.

To test this hypothesis, we had our three subjects perform a contrast matching psychophysical experiment, using the same stimuli that were used for the eye movement recordings. The experiment was in the form of a two-interval forced choice (2IFC): Two stimuli were presented in succession for 170 ms each, separated by a short interval during which the screen was blank. Subjects had then to report which interval contained the stimulus with higher perceived contrast. During one

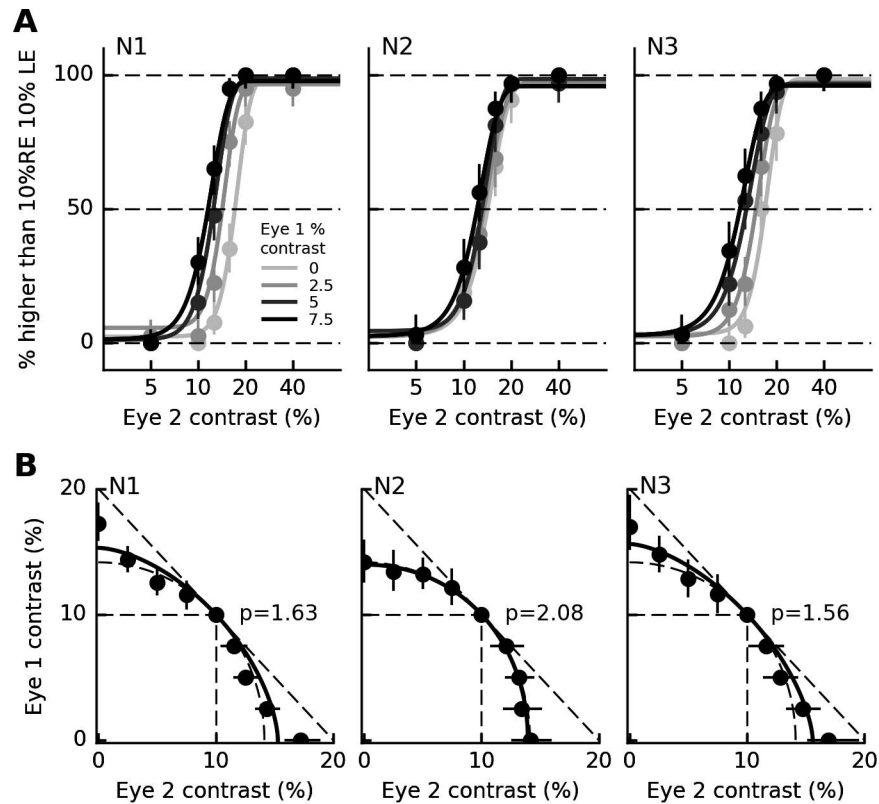


Figure 5. Perception of dichoptic gratings. (A) Subjects compared the contrast of a binocular stimulus (10% contrast in each eye) to that of stimuli in which the contrast was different in the two eyes (dichoptic stimuli). For dichoptic stimuli, the stimulus in one eye had one of four contrast levels, corresponding to each of the four curves, whereas the contrast seen by the other eye varied over a broad range. As contrast in one eye was lowered, a higher contrast in the other eye was required to achieve a perceptual match with the binocular standard. Both mean and *SEM* bars for the data are shown. (B) Dichoptic contrasts that yielded the same perceived contrast are shown, based on the fits to the data in A. Fits using the power summation rule are shown. The value of the only parameter p is also shown. The dashed lines highlight values of p of particular significance, corresponding to linear summation (diagonal), Pythagorean sum (circle), and winner-take-all (square) binocular combination rules.

of the two intervals a 10% contrast binocular grating (reference stimulus) was shown; during the other interval a grating with one of four contrast levels (0, 2.5, 5, or 7.5%) was shown to one eye (eye 1, which in different trials could be either the left or the right eye) and an identical grating with one of six contrast levels (5, 10, 12.6, 15.88, 20, or 40%) was shown to the other eye (eye 2). In Figure 5A we plot, for the three subjects, the percentage of times that the reference stimulus was reported to have lower contrast. A separate psychometric curve was fitted for each of the four contrast levels in eye 1. Slight left/right eye asymmetries were averaged by pooling the data regardless of whether eye 1 was the left or the right eye in a given trial. As expected, when the contrast shown to eye 1 decreased, the point at which the corresponding psychometric curve crossed 50% (i.e., the contrast that needed to be shown to eye 2 to match the perceived contrast of the reference stimulus) increased. However, even with monocular stimuli (zero eye 1 contrast), this point never reached 20%.

In Figure 5B this same data are plotted in a different format, one which is routinely used in the psychophysical literature. Here points that have the same apparent contrast, based on the fits shown in Figure 2A, are shown, together with a fit using the power summation rule (Legge & Rubin, 1981):

$$2c_{BE}^p = c_{RE}^p + c_{LE}^p$$

This equation has a single parameter, the exponent p , and in our experiments c_{BE} was always equal to 10%. Three values of p are particularly meaningful. When $p = 1$ (diagonal dashed line) the perceived contrast is equal to the linear sum of the contrasts from the two eyes; when $p = 2$ (dashed circle) perceived contrast is determined by the Pythagorean sum of the contrasts from the two eyes (quadratic summation); finally, when $p = \infty$ (dashed square at 10% contrast), perceived contrast is equal to the highest contrast in the two eyes. In our three subjects, the best fitting p (shown in each panel) is between 1.5 and 2. This is within the range of values reported in previous psychophysical studies

(Legge & Rubin, 1981; Legge, 1984b; Anderson & Movshon, 1989; Meese et al., 2006).

Importantly, this experiment allowed us to determine monocular and binocular stimuli that were perceived as having the same contrast. The binocular stimulus always had 10% contrast in each eye (the reference stimulus), whereas the perceptually equivalent monocular stimulus varied across subjects: It was 17.2% in N1, 14.2% in N2, and 16.9% in N3. Armed with these results we can now go back to our eye movement recordings, and find the magnitude of the OFRs corresponding to these stimuli, which are indicated with black square symbols in Figure 2. These stimuli obviously induced vastly different OFRs, despite being perceptually equivalent. The ratio between the OFRs induced by the perceptually equivalent binocular and monocular stimuli is 2.24 in N1, 2.25 in N2, and 2.44 in N3. It thus appears that perception and ocular following rely on at least partially distinct neuronal substrates, which combine binocular inputs according to different rules.

Binocular summation with 1D noise gratings: OFRs

In the binocular conditions tested above, the eyes saw two identical stimuli. It has been reported that when the two eyes see sinusoidal gratings that have different phases, they are perceived as having lower contrast than when they have the same phase, especially when the contrast of the stimuli is low and the phase difference is large (Westendorf & Fox, 1974; Bacon, 1976; Blake & Rush, 1980; Green & Blake, 1981; Baker, Wallis, Georgeson, & Meese, 2012). This finding might be related to the observation that the response of most binocular neurons in visual cortex is sensitive to the interocular phase of the binocular inputs (Poggio & Fischer, 1977; Ohzawa & Freeman, 1986; Gonzalez & Perez, 1998; Cumming & DeAngelis, 2001). It would thus be interesting to test how interocular phase differences affect the OFRs. It has already been shown that applying a disparity to a stimulus causes a modest attenuation of the OFRs (Masson, Busetini, Yang, & Miles, 2001), but the presence of a disparity also triggers a short latency disparity vergence response (Busettini, Masson, & Miles, 1996; Busettini, Miles, & Krauzlis, 1996), potentially contaminating the measure. By using noise stimuli it is however possible to manipulate interocular correlation between the two eyes without inducing significant vergence responses. This can be achieved by simply presenting different (i.e., uncorrelated) noise stimuli to the two eyes.

We presented random line stimuli (RLS) spanning a range of RMS contrasts to our three subjects. The stimuli always drifted up or down at high speed, and

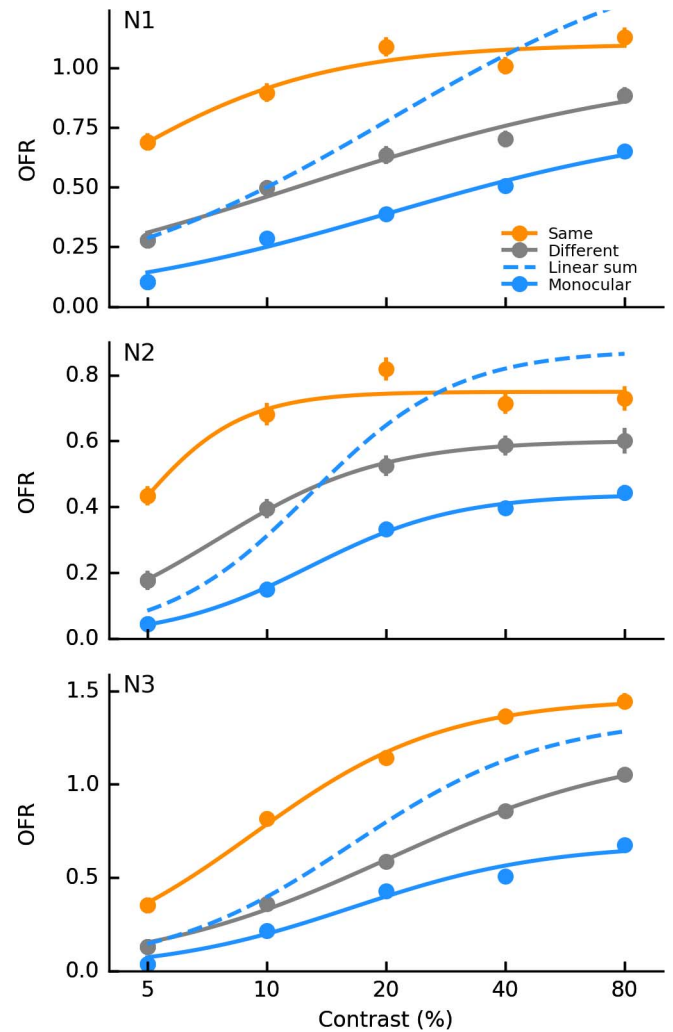


Figure 6. Contrast tuning of OFRs to monocular and binocular drifting noise gratings. As with sinusoidal gratings (Figure 2), OFRs increased monotonically with the contrast of 1D noise stimuli, and saturated at intermediate and high contrasts. At all contrasts, presenting the same stimulus to both eyes (orange) yielded larger responses than monocular stimuli (solid blue), usually more than twice as large (dashed blue). OFRs recorded when different (uncorrelated) noise patterns (of the same contrast) were presented to the two eyes (gray) fell in the middle. Both mean and *SEM* bars are shown. Naka–Rushton fits to the data are shown; values for the parameters and goodness-of-fit measures are listed in Table 1.

were presented either to only one eye or to both eyes. In binocular presentations the two eyes saw either the same stimulus, or two different RLS (drifting at the same speed and in the same direction). As we did before, we identified the open-loop time window for each subject, and used the latencies of the OFRs elicited in the binocular-same conditions to time-shift the responses as a function of contrast. The relationship between contrast and the OFR in our three subjects is shown in Figure 6, separately for monocular (blue),

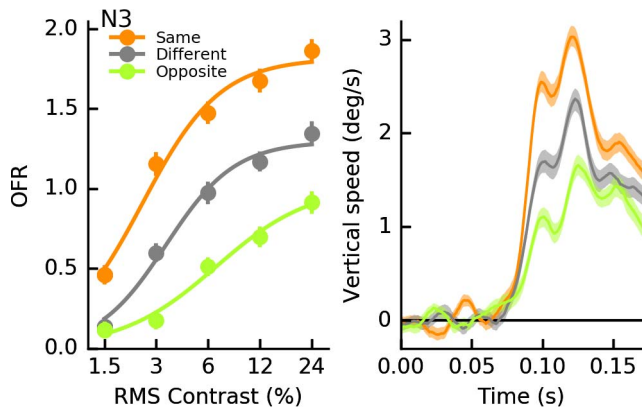


Figure 7. OFRs to binocular low-pass filtered drifting noise gratings. (A) As seen in Figure 6, OFRs increased monotonically with the RMS contrast of low-pass filtered 1D noise stimuli, saturating at high contrasts. At all contrasts, OFRs were larger when the same stimulus was shown to both eyes (orange), than when different (uncorrelated) stimuli were (gray). When binocular-opposite (anti-correlated) stimuli were presented (green), the responses were even weaker. Both mean and *SEM* bars are shown. Naka–Rushton fits to the data are shown; values for the parameters and goodness-of-fit measures are listed in Table 1. (B) Time course of the response to 24% RMS contrast binocular-same (orange), binocular-different (gray), and binocular-opposite (green) stimuli. Both the mean (solid line) and the *SEM* (shaded region, estimated using bootstrap-based methods) are shown. Binocular-same and binocular-opposite stimuli became significantly different ($p < 0.05$) starting 83 ms after stimulus onset, 10 ms after the onset of responses to binocular-same stimuli.

binocular-same (orange), and binocular-different (gray) stimuli. Also shown are fits of Naka–Rushton functions to the data (parameter values and goodness-of-fit measures are listed in Table 1) and the linear-summation prediction. There was more variability across subjects than in the experiment with sinusoidal gratings, possibly due to a different sensitivity of each subject to the various SF present in the noise stimulus, and in two subjects the ratio between responses to binocular-same and monocular stimuli fell below 2 at high contrast (dashed blue curve). The critical finding from this experiment is however that, at all contrasts, responses to binocular-different stimuli were smaller than those induced by binocular-same stimuli, although still larger than those induced by monocular stimuli. This suggests that the neurons that mediate OFRs are sensitive to interocular correlation (i.e., binocular disparity). The model presented above is thus a simplification; a model based on disparity tuned binocular neurons at the second stage is necessary to account for these data. This could be accomplished by simply making the gain G of the second stage a function of interocular phase. For example, one could postulate that the binocular stage of processing is mediated by

neurons tuned to zero disparity, as proposed by others to account for the effect of interocular phase in perceptual binocular summation (Baker et al., 2012). Such neurons would produce maximal responses for binocular-same stimuli and weaker responses for binocular-different (uncorrelated) stimuli (Cumming & Parker, 1997), just as we observed.

Because neurons tuned to zero disparity typically produce (Cumming & Parker, 1997) even weaker responses to anticorrelated stimuli (i.e., stimuli obtained by presenting contrast-reversed, but otherwise identical, images to the two eyes), we further tested this hypothesis by presenting anti-correlated stimuli to one of our subjects. In this experiment low-pass filtered RLS stimuli were used, and three interocular binocular correlation conditions were tested: binocular-same, binocular-different (i.e., uncorrelated), and binocular-opposite (i.e., anticorrelated). We found (Figure 7A; parameter values and goodness-of-fit measures for the fits are listed in Table 1) that once again binocular-different stimuli (gray) induced weaker responses than binocular-same stimuli (orange), at all contrasts; importantly, binocular-opposite stimuli (green) induced even weaker OFRs. At high-contrast, the ratio between binocular-same and binocular-opposite OFRs was slightly larger than 2, indicating that binocular-opposite stimuli were probably as effective as monocular stimuli (which were not included in this experiment).

This last observation suggests a potential alternative interpretation for our results: Responses to stimuli that are different in the two eyes might be weaker as a result of binocular rivalry (Blake & Wilson, 2011), which might suppress the input from one eye. Rivalry might be expected to be proportional to the difference between the images presented to the two eyes, and thus could be stronger for binocular-opposite stimuli (in which all lines have opposite contrast) than for binocular-different stimuli (in which, on average, only half of the lines are different). While intuitively attractive, this explanation does not stand up to scrutiny. First, the stimuli used in this experiment did not appear perceptually rivalrous. This is not surprising, given that the RLS presented to the two eyes had the same orientation, spatial frequency content, and drifted at the same speed. Second, it is well-known that rivalry takes time to ensue. Rivalry onset is usually estimated to take anywhere between 150 and 450 ms from stimulus onset (Wolfe, 1983; Blake, 1989), although recording OFRs to stimuli that differ in the two eyes in terms of both orientation and temporal frequency content, and are perceptually rivalrous, we have reported that the first signs of rivalry could actually appear as early as 110 ms from stimulus onset (Quaia, Optican, & Cumming, 2016). If we examine the time course of the OFRs induced by 24% RMS contrast

stimuli in our experiment (Figure 7B) we find however that the three classes of stimuli induced different responses from the very beginning. For example, binocular-same stimuli induced a response that became significantly different from zero ($p < 0.05$) 73 ms after stimulus onset, and was already significantly larger than that induced by binocular-opposite stimuli only 10 ms later (83 ms from stimulus onset). This is at least 30 ms faster than any rivalry onset estimate we know of.

Discussion

We characterized binocular summation (the response boost conferred by binocular over monocular stimulation) for ocular following eye movements, across a wide range of supra-threshold contrast levels. We discovered that, for OFRs, binocular summation is large at all contrasts when the two eyes are presented with identical stimuli, but is smaller when uncorrelated (or anticorrelated) stimuli are shown to the two eyes. Differences between monocular and binocular OFRs to high contrast drifting random-dot stimuli had been reported before in monkeys, but only qualitatively and without a characterization of the sensitivity of binocular summation to contrast and interocular phase differences (Miles et al., 1986; Inoue et al., 2000). A modest dependency of the OFR on the absolute disparity of a high-contrast noise stimulus has been previously reported (Masson et al., 2001), but those results were potentially contaminated by short latency vergence responses.

As noted in the Introduction, sizable binocular summation for perception has been observed only at very low contrasts, at or just above threshold. Binocular summation is thus quite different for perception and OFRs, adding it to the list of phenomena that exhibit different properties when evaluated using perception and eye movements (Bostrom & Warzecha, 2010; Simoncini, Perrinet, Montagnini, Mamassian, & Masson, 2012; Blum & Price, 2014; Glasser & Tadin, 2014; Price & Blum, 2014; Quaia et al., 2016). It is generally difficult to pinpoint the source of such differences, especially when perception and eye movements are measured using stimuli that differ in their spatiotemporal content. However, by directly comparing OFRs to monocular and binocular stimuli having identical perceived contrast (Figure 2), we ruled out this source of uncertainty. A possible explanation for this large difference is that OFRs might rely only on a small subset of V1 neurons, which might not be representative of the neurons involved in perception. First, only direction-selective (DS) neurons, which are approximately 20% of all V1 neurons (De Valois, Yund, & Hepler, 1982; Orban, Kennedy, &

Bullier, 1986; Hawken, Parker, & Lund, 1988; Gur, Kagan, & Snodderly, 2005), can contribute to a directional response. Second, the OFR is tuned to low spatial frequencies and high temporal frequencies (i.e., high speeds), which strongly activate only a subset of DS neurons in V1 (mostly part of the magnocellular pathway). Finally, our results with noise stimuli indicate that OFRs might be dominated by neurons tuned to zero or near-zero disparity, again a subset of V1 neurons. This might explain why recording methods that are sensitive to the pooled activity of large populations of V1 neurons, such as fMRI (Moradi & Heeger, 2009) and EEG (Baker & Wade, 2017), find limited binocular summation, more in line with perceptual reports than with OFRs. Both these measures and perceptual contrast judgments might be dominated by parvocellular signals, with little regard for direction selectivity, speed preference, and preferred disparity. This is sensible, since it is reasonable to expect that, when carrying out perceptual contrast matching, a subject would rely mostly on parvocellular neurons, which encode contrast linearly, instead of magnocellular signals, which quickly saturate with contrast (Derrington & Lennie, 1984; Kaplan & Shapley, 1986; Sclar et al., 1990; Usrey & Reid, 2000; Alitto et al., 2011). OFRs instead are known to be mediated by neurons in areas MT and MST (Takemura et al., 2007; Masson & Perrinet, 2012), whose activity is in turn determined mostly by magnocellular LGN neurons (Maunsell, Nealey, & DePriest, 1990), and accordingly saturate quickly with contrast.

A simple two-stage model, compatible with what is known about the dorsal stream of visual processing, accounted very well for the OFRs induced by monocular and binocular sinusoidal gratings (Figure 4). Extending it by making its second stage tuned to zero-disparity would allow it to also account for the effect of inter-ocular phase differences seen with our noise stimuli (Figures 6 and 7). One limit of this explanation is that, whereas neurons tuned to zero-disparity are present in significant numbers in cortical area V1 (Cumming & DeAngelis, 2001; Prince, Cumming, & Parker, 2002), they appear to be conspicuously rare in extrastriate visual areas MT and MST (DeAngelis & Newsome, 1999; Takemura, Inoue, Kawano, Quaia, & Miles, 2001; Cumming & DeAngelis, 2001), which are known to mediate OFRs (Takemura et al., 2007). One possible explanation is that the disparity tuning to flashed and drifting stimuli might be different, but the available evidence argues against this interpretation (Anzai, Ohzawa, & Freeman, 2001; Palanca & DeAngelis, 2003). Alternatively, we can only speculate that the region of MST from which these neurons have been recorded is not the same as the one that drives OFRs, where perhaps zero-disparity tuned neurons might be found. Since our

results indicate that only neurons that respond more strongly to binocular-same than to binocular-different (or binocular-opposite) stimuli are good candidates for driving OFRs, this is obviously an important subject for future electrophysiological studies.

Acknowledgments

This research was supported by the Intramural Research Program of the National Eye Institute, NIH, DHHS. We thank Boris Sheliga for assistance in running the experiments.

Commercial relationships: none.

Corresponding author: Christian Quaia.

Email: quaiaac@nei.nih.gov.

Address: Laboratory of Sensorimotor Research, National Eye Institute, National Institutes of Health, Department of Health and Human Services, Bethesda, MD, USA.

References

- Albrecht, D., & Geisler, W. (1991). Motion selectivity and the contrast-response function of simple cells in the visual cortex. *Visual Neuroscience*, 7, 531–546.
- Alitto, H., Moore, B., Rathbun, D., & Usrey, W. (2011). A comparison of visual responses in the lateral geniculate nucleus of alert and anaesthetized macaque monkeys. *Journal of Physiology*, 589, 87–99.
- Alitto, H., & Usrey, W. (2008). Origin and dynamics of extraclassical suppression in the lateral geniculate nucleus of the macaque monkey. *Neuron*, 57, 135–146.
- Anderson, P., & Movshon, J. (1989). Binocular combination of contrast signals. *Vision Research*, 29, 1115–1132.
- Anzai, A., Ohzawa, I., & Freeman, R. (2001). Joint-encoding of motion and depth by visual cortical neurons: Neural basis of the Pulfrich effect. *Nature Neuroscience*, 4, 513–518.
- Arditi, A., Anderson, P., & Movshon, J. (1981). Monocular and binocular detection of moving sinusoidal gratings. *Vision Research*, 21, 329–36.
- Bacon, J. (1976). The interaction of dichoptically presented spatial gratings. *Vision Research*, 16, 337–344.
- Baker, D., Meese, T., & Georgeson, M. (2007). Binocular interaction: Contrast matching and contrast discrimination are predicted by the same model. *Spatial Vision*, 20, 397–413.
- Baker, D., & Wade, A. (2017). Evidence for an optimal algorithm underlying signal combination in human visual cortex. *Cerebral Cortex*, 27, 254–264.
- Baker, D., Wallis, S., Georgeson, M., & Meese, T. (2012). The effect of interocular phase difference on perceived contrast. *PLoS One*, 7, e34696.
- Barlow, H., Blakemore, C., & Pettigrew, J. (1967). The neural mechanism of binocular depth discrimination. *Journal of Physiology*, 193, 327–342.
- Barthelemy, F., Perrinet, L., Castet, E., & Masson, G. (2008). Dynamics of distributed 1D and 2D motion representations for short-latency ocular following. *Vision Research*, 48, 501–522.
- Benardete, E., Kaplan, E., & Knight, B. (1992). Contrast gain control in the primate retina: P cells are not X-like, some M cells are. *Visual Neuroscience*, 8, 483–486.
- Blake, R. (1989). A neural theory of binocular rivalry. *Psychological Review*, 96, 145–167.
- Blake, R., & Rush, C. (1980). Temporal properties of binocular mechanisms in the human visual system. *Experimental Brain Research*, 38, 333–340.
- Blake, R., & Wilson, H. (2011). Binocular vision. *Vision Research*, 51, 754–770.
- Blum, J., & Price, N. (2014). Reflexive tracking eye movements and motion perception: One or two neural populations? *Journal of Vision*, 14(3):23, 1–14, <https://doi.org/10.1167/14.3.23>. [PubMed] [Article]
- Bostrom, K., & Warzecha, A. (2010). Open-loop speed discrimination performance of ocular following response and perception. *Vision Research*, 50, 870–882.
- Brainard, D. (1997). The Psychophysics Toolbox. *Spatial Vision*, 10, 433–436.
- Busettoni, C., Masson, G., & Miles, F. (1996, March 28). A role for stereoscopic depth cues in the rapid visual stabilization of the eyes. *Nature*, 380, 342–345.
- Busettoni, C., Miles, F., & Krauzlis, R. (1996). Short-latency disparity vergence responses and their dependence on a prior saccadic eye movement. *Journal of Neurophysiology*, 75, 1392–1410.
- Cagenello, R., Arditi, A., & Halpern, D. (1993). Binocular enhancement of visual acuity. *Journal of the Optical Society of America. A, Optics, Image Science, and Vision*, 10, 1841–1848.
- Camp, A., Tailby, C., & Solomon, S. (2009). Adaptable mechanisms that regulate the contrast response of

- neurons in the primate lateral geniculate nucleus. *Journal of Neuroscience*, *29*, 5009–5021.
- Campbell, F., & Green, D. (1965, October 9). Monocular versus binocular visual acuity. *Nature*, *208*, 191–192.
- Collewijn, H., van der Mark, F., & Jansen, T. (1975). Precise recording of human eye movements. *Vision Research*, *15*, 447–450.
- Cumming, B., & DeAngelis, G. (2001). The physiology of stereopsis. *Annual Review of Neuroscience*, *24*, 203–238.
- Cumming, B., & Parker, A. (1997, September 18). Responses of primary visual cortical neurons to binocular disparity without depth perception. *Nature*, *389*, 280–283.
- De Valois, R., Yund, E., & Hepler, N. (1982). The orientation and direction selectivity of cells in macaque visual cortex. *Vision Research*, *22*, 531–544.
- DeAngelis, G., & Newsome, W. (1999). Organization of disparity-selective neurons in macaque area MT. *Journal of Neuroscience*, *19*, 1398–1415.
- DeAngelis, G., & Newsome, W. (2004). Perceptual 'read-out' of conjoined direction and disparity maps in extrastriate area MT. *PLoS Biology*, *2*, E77.
- Derrington, A., & Lennie, P. (1984). Spatial and temporal contrast sensitivities of neurones in lateral geniculate nucleus of macaque. *Journal of Physiology*, *357*, 219–240.
- Ding, J., & Sperling, G. (2006). A gain-control theory of binocular combination. *Proceedings of the National Academy of Sciences USA*, *103*, 1141–1146.
- Efron, B. (1982). *The jackknife, the bootstrap, and other resampling plans*. Philadelphia: SIAM.
- Gellman, R., Carl, J., & Miles, F. (1990). Short latency ocular-following responses in man. *Visual Neuroscience*, *5*, 107–122.
- Glasser, D., & Tadin, D. (2014). Modularity in the motion system: Independent oculomotor and perceptual processing of brief moving stimuli. *Journal of Vision*, *14*(3):28, 1–13, <https://doi.org/10.1167/14.3.28>. [PubMed] [Article]
- González, E., Lillakas, L., Greenwald, N., Gallie, B., & Steinbach, M. (2014). Unaffected smooth pursuit but impaired motion perception in monocularly enucleated observers. *Vision Research*, *101*, 151–157.
- Gonzalez, F., & Perez, R. (1998). Neural mechanisms underlying stereoscopic vision. *Progress in Neurobiology*, *55*, 191–224.
- Green, M., & Blake, R. (1981). Phase effects in monoptic and dichoptic temporal integration: Flicker and motion detection. *Vision Research*, *21*, 365–372.
- Gur, M., Kagan, I., & Snodderly, D. (2005). Orientation and direction selectivity of neurons in V1 of alert monkeys: Functional relationships and laminar distributions. *Cerebral Cortex*, *15*, 1207–1221.
- Hawken, M., Parker, A., & Lund, J. (1988). Laminar organization and contrast sensitivity of direction-selective cells in the striate cortex of the old world monkey. *Journal of Neuroscience*, *8*, 3541–3548.
- Hays, A., Richmond, B., & Optican, L. (1982). A UNIX-based multiple process system for real-time data acquisition and control. In *Wescon conference proceedings* (p. 1–10).
- Hess, R., Hutchinson, C., Ledgeway, T., & Mansouri, B. (2007). Binocular influences on global motion processing in the human visual system. *Vision Research*, *47*, 1682–1692.
- Inoue, Y., Takemura, A., Kawano, K., & Mustari, M. (2000). Role of the pretectal nucleus of the optic tract in short-latency ocular following responses in monkeys. *Experimental Brain Research*, *131*, 269–281.
- Kaplan, E., & Shapley, R. (1986). The primate retina contains two types of ganglion cells, with high and low contrast sensitivity. *Proceedings of the National Academy of Sciences USA*, *83*, 2755–2757.
- Kawano, K. (1999). Ocular tracking: Behavior and neurophysiology. *Current Opinion in Neurobiology*, *9*, 467–473.
- Kingdom, F., & Libenson, L. (2015). Dichoptic color saturation mixture: Binocular luminance contrast promotes perceptual averaging. *Journal of Vision*, *15*(5):2, <https://doi.org/10.1167/15.5.2>. [PubMed] [Article]
- Krauskopf, J., Cornsweet, T., & Riggs, L. (1960). Analysis of eye movements during monocular and binocular fixation. *Journal of the Optical Society of America*, *50*, 572–578.
- Kremers, J., Silveira, L., & Kilavik, B. (2001). Influence of contrast on the responses of marmoset lateral geniculate cells to drifting gratings. *Journal of Neurophysiology*, *85*, 235–246.
- Kukkonen, H., Rovamo, J., Tiippana, K., & Näsänen, R. (1993). Michelson contrast, RMS contrast and energy of various spatial stimuli at threshold. *Vision Research*, *33*, 1431–1436.
- Legge, G. (1984a). Binocular contrast summation. I. Detection and discrimination. *Vision Research*, *24*, 373–383.

- Legge, G. (1984b). Binocular contrast summation. II. Quadratic summation. *Vision Research*, *24*, 385–394.
- Legge, G., & Rubin, G. (1981). Binocular interactions in suprathreshold contrast perception. *Perceptions in Psychophysics*, *30*, 49–61.
- Masson, G. (2004). From 1D to 2D via 3D: Dynamics of surface motion segmentation for ocular tracking in primates. *Journal of Physiology Paris*, *98*, 35–52.
- Masson, G., Busettoni, C., Yang, D., & Miles, F. (2001). Short-latency ocular following in humans: Sensitivity to binocular disparity. *Vision Research*, *41*, 3371–3387.
- Masson, G., & Perrinet, L. (2012). The behavioral receptive field underlying motion integration for primate tracking eye movements. *Neuroscience and Biobehavioral Reviews*, *36*, 1–25.
- Maunsell, J., Nealey, T., & DePriest, D. (1990). Magnocellular and parvocellular contributions to responses in the middle temporal visual area (MT) of the macaque monkey. *Journal of Neuroscience*, *10*, 3323–3334.
- Meese, T., Georgeson, M., & Baker, D. (2006). Binocular contrast vision at and above threshold. *Journal of Vision*, *6*(11):7, 1224–1243, <https://doi.org/10.1167/6.11.7>. [PubMed] [Article]
- Miles, F. (1997). Visual stabilization of the eyes in primates. *Current Opinion in Neurobiology*, *7*, 867–871.
- Miles, F. (1998). The neural processing of 3-D visual information: Evidence from eye movements. *European Journal of Neuroscience*, *10*, 811–822.
- Miles, F., Busettoni, C., Masson, G., & Yang, D. (2004). Short-latency eye movements: Evidence for rapid, parallel processing of optic flow. In L. Vaina, S. Beardsley, & S. Rushton (Eds.), *Optic flow and beyond*, (pp. 79–107). Dordrecht, The Netherlands: Kluwer Academic Press.
- Miles, F., Kawano, K., & Optican, L. (1986). Short-latency ocular following responses of monkey. I. Dependence on temporospatial properties of visual input. *Journal of Neurophysiology*, *56*, 1321–1354.
- Miura, K., Matsuura, K., Taki, M., Tabata, H., Inaba, N., Kawano, K., & Miles, F. (2006). The visual motion detectors underlying ocular following responses in monkeys. *Vision Research*, *46*, 869–878.
- Moradi, F., & Heeger, D. (2009). Inter-ocular contrast normalization in human visual cortex. *Journal of Vision*, *9*(3):13, 1–22, <https://doi.org/10.1167/9.3.13>. [PubMed] [Article]
- Moulden, B., Kingdom, F., & Gatley, L. (1990). The standard deviation of luminance as a metric for contrast in random-dot images. *Perception*, *19*, 79–101.
- Ohzawa, I., & Freeman, R. (1986). The binocular organization of simple cells in the cat's visual cortex. *Journal of Neurophysiology*, *56*, 221–242.
- Orban, G., Kennedy, H., & Bullier, J. (1986). Velocity sensitivity and direction selectivity of neurons in areas V1 and V2 of the monkey: Influence of eccentricity. *Journal of Neurophysiology*, *56*, 462–480.
- Palanca, B., & DeAngelis, G. (2003). Macaque middle temporal neurons signal depth in the absence of motion. *Journal of Neuroscience*, *23*, 7647–7658.
- Pettigrew, J., Nikara, T., & Bishop, P. (1968). Binocular interaction on single units in cat striate cortex: Simultaneous stimulation by single moving slit with receptive fields in correspondence. *Experimental Brain Research*, *6*, 391–410.
- Pineles, S., Velez, F., Yu, F., Demer, J., & Birch, E. (2014). Normative reference ranges for binocular summation as a function of age for low contrast letter charts. *Strabismus*, *22*, 167–175.
- Poggio, G., & Fischer, B. (1977). Binocular interaction and depth sensitivity in striate and prestriate cortex of behaving rhesus monkey. *Journal of Neurophysiology*, *40*, 1392–1405.
- Price, N., & Blum, J. (2014). Motion perception correlates with volitional but not reflexive eye movements. *Neuroscience*, *277*, 435–445.
- Priebe, N., & Ferster, D. (2006). Mechanisms underlying cross-orientation suppression in cat visual cortex. *Nature Neuroscience*, *9*, 552–561.
- Prince, S., Cumming, B., & Parker, A. (2002). Range and mechanism of encoding of horizontal disparity in macaque V1. *Journal of Neurophysiology*, *87*, 209–221.
- Prince, S., Pointon, A., Cumming, B., & Parker, A. (2002). Quantitative analysis of the responses of V1 neurons to horizontal disparity in dynamic random-dot stereograms. *Journal of Neurophysiology*, *87*, 191–208.
- Quaia, C., Optican, L., & Cumming, B. (2013). Terminator disparity contributes to stereo matching for eye movements and perception. *Journal of Neuroscience*, *33*, 18867–18879.
- Quaia, C., Optican, L., & Cumming, B. (2016). A motion-from-form mechanism contributes to extracting pattern motion from plaids. *Journal of Neuroscience*, *36*, 3903–3918.
- Quaia, C., Sheliga, B., Fitzgibbon, E., & Optican, L. (2012). Ocular following in humans: Spatial prop-

- erties. *Journal of Vision*, 12(4):13, 1–29. <https://doi.org/10.1167/12.4.13>. [PubMed] [Article]
- Quaia, C., Sheliga, B., Optican, L., & Cumming, B. (2013). Temporal evolution of pattern disparity processing in humans. *Journal of Neuroscience*, 33, 3465–3476.
- Robinson, D. (1963). A method of measuring eye movement using a scleral search coil in a magnetic field. *IEEE Transactions on Biomedical Engineering*, 10, 137–145.
- Rose, D. (1980). The binocular: Monocular sensitivity ratio for movement detection varies with temporal frequency. *Perception*, 9, 577–580.
- Sclar, G., Maunsell, J., & Lennie, P. (1990). Coding of image contrast in central visual pathways of the macaque monkey. *Vision Research*, 30, 1–10.
- Shanidze, N., Heinen, S., & Verghese, P. (2017). Monocular and binocular smooth pursuit in central field loss. *Vision Research*, 141, 181–190.
- Sheliga, B., Chen, K., Fitzgibbon, E., & Miles, F. (2005). Initial ocular following in humans: A response to first-order motion energy. *Vision Research*, 45, 3307–3321.
- Simoncini, C., Perrinet, L., Montagnini, A., Mamasian, P., & Masson, G. (2012). More is not always better: Adaptive gain control explains dissociation between perception and action. *Nature Neuroscience*, 15, 1596–1603.
- Solomon, S., Lee, B., & Sun, H. (2006). Suppressive surrounds and contrast gain in magnocellular-pathway retinal ganglion cells of macaque. *Journal of Neuroscience*, 26, 8715–8726.
- Solomon, S., White, A., & Martin, P. (2002). Extraclassical receptive field properties of parvocellular, magnocellular, and koniocellular cells in the primate lateral geniculate nucleus. *Journal of Neuroscience*, 22, 338–349.
- Takemura, A., Inoue, Y., Kawano, K., Quaia, C., & Miles, F. (2001). Single-unit activity in cortical area MST associated with disparity-vergence eye movements: Evidence for population coding. *Journal of Neurophysiology*, 85, 2245–2266.
- Takemura, A., Murata, Y., Kawano, K., & Miles, F. (2007). Deficits in short-latency tracking eye movements after chemical lesions in monkey cortical areas MT and MST. *Journal of Neuroscience*, 27, 529–541.
- Taki, M., Miura, K., Tabata, H., Hisa, Y., & Kawano, K. (2009). The effects of prolonged viewing of motion on short-latency ocular following responses. *Experimental Brain Research*, 195, 195–205.
- Usrey, W., & Reid, R. (2000). Visual physiology of the lateral geniculate nucleus in two species of new world monkey: *Saimiri sciureus* and *Aotus trivirgatus*. *Journal of Physiology*, 523, 755–769.
- Webb, B., Tinsley, C., Barraclough, N., Easton, A., Parker, A., & Derrington, A. (2002). Feedback from V1 and inhibition from beyond the classical receptive field modulates the responses of neurons in the primate lateral geniculate nucleus. *Visual Neuroscience*, 19, 583–592.
- Westendorf, D., & Fox, R. (1974). Binocular detection of positive and negative flashes. *Perceptions in Psychophysics*, 15, 61–65.
- Wolfe, J. (1983). Influence of spatial frequency, luminance, and duration on binocular rivalry and abnormal fusion of briefly presented dichoptic stimuli. *Perception*, 12, 447–456.
- Zlatkova, M., Anderson, R., & Ennis, F. (2001). Binocular summation for grating detection and resolution in foveal and peripheral vision. *Vision Research*, 41, 3093–3100.